

# Evolutionary Singularity Filter Bank Optimization for Fingerprint Image Enhancement

Ung-Keun Cho, Jin-Hyuk Hong, and Sung-Bae Cho

Dept. of Computer Science, Yonsei University,  
Biometrics Engineering Research Center,  
134 Sinchon-dong, Seodaemun-ku,  
Seoul 120-749, Korea  
{bearroot, hjinh}@sclab.yonsei.ac.kr,  
sbcho@cs.yonsei.ac.kr

**Abstract.** Singularity is the special feature of fingerprints for identification and classification. Since the performance of singularity extraction depends on the quality of fingerprint images, image enhancement is required to improve the performance. Image enhancement with various image filters might be more useful than a filter, but it is very difficult to find a set of appropriate filters. In this paper, we propose a method that uses the genetic algorithm to find those filters for superior performance of singularity extraction. The performance of the proposed method has been verified by the experiment with NIST DB 4. Moreover, the proposed method does not need any expert knowledge to find the type and order of filters for the target domain, it can be easily applied to other applications of image processing.

## 1 Introduction

AFIS (Automatic Fingerprint Identification System) finds out whether an individual's incoming fingerprint image is the same as any of the target templates in the database. Classification, which groups fingerprints into predefined several categories based on the basis of global ridge pattern, can reduce the number of fingerprints for matching in the large database. Singular points are conceptualized as aid for fingerprint classification by Henry [1], and used for better identification [2]. The accuracy of singularity extraction is subject to the quality of images, so that it is hard to achieve good performance. There are lots of methods for singularity extraction but also the improvement of the quality [3].

Segmentation [4] and enhancement [5] to improve the quality of fingerprint images. Segmentation classifies a part of the image into a background or fingerprint region, so as to discard the background regions to reduce the number of false features extracted. Enhancement improves the clarity of the ridge structures to extract correct features. There are many filters for enhancement. For fingerprint images, enhancement using various filters together might be better than when using only one, but usually it requires the expert knowledge to determine the type and order of filters [5,6,7,8].

Since it is actually impossible to examine all possible combinations of filters, it needs a heuristic algorithm. In this paper, we exploit the genetic algorithm [9,10,11,12] to find out a set of proper filters to enhance the fingerprint images.

## 2 Related Work

### 2.1 Singularity

Fingerprints contain singularities that are known as core and delta points. The core is the topmost point on the innermost recurving ridge, while the delta is the center of a triangular region where three different direction flows meet. In the process of fingerprint classification, singularity is used directly [13], or with ridge patterns [14,15]. It was also used as landmarks for the other features [16,17]. There are other applications of singularity such as landmarks for fingerprint matching [18].

The Poincare index is a popular method to detect singularity using orientation field [3]. Fig. 1 shows the orientation field of core and delta regions. The orientation field is estimated for each block, and it is subject to the quality of the image. Image enhancement to improve the quality is required to calculate the orientation field correctly.

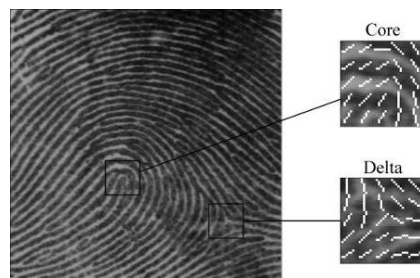


Fig. 1. The orientation field of core and delta regions

### 2.2 Image Filter

The goal of general image processing is to detect objects on image and to classify them through the analysis of images. In images, low quality is hard to correctly extract features. Filtering, such as reducing image noises, smoothing, removing some forms of misfocus and motion blur, is in the front step of image processing. Typically, there are histogram-based, mask-based and morphology-based image filters [19]. Many methods have used these filters to improve quality of fingerprint image. Since Hong [5] introduced the Gabor filter to enhance fingerprint images, it has been adopted in many methods for fingerprint enhancement [6,7,8]. Fig. 2 shows example images obtained by several filters.

### 2.3 Genetic Algorithm

The genetic algorithm is an evolutionary algorithm, which is based on mechanisms of natural selection and the survival of fittest. In each generation, a new set of individuals

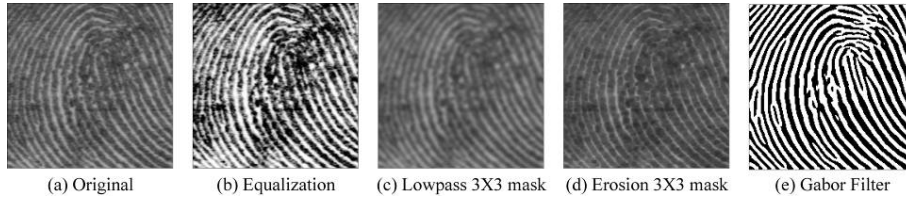


**Fig. 2.** Example images after filtering

is generated by selection, crossover, and mutation of previous ones. An individual represents a solution to the problem by a list of parameters, called chromosome or genome. The first population, a set of chromosomes, is initialized randomly, while population in the next generation is generated from population of the previous generation. The population is stochastically generated using genetic operators such as selection, crossover, and mutation with the fitness measures of current population. Generally the average fitness will have increased by this procedure for the population. The genetic algorithm has been successfully applied in many search, optimization, and machine learning problems [9,10].

### 3 Image Enhancement Based on Genetic Algorithm

For the correct feature extraction, the quality of the image should be improved by using appropriate image filters. The number of constructing an ordered subset of  $n$  filters from a set of  $m$  filters is given by  $m^n$ . Trying all cases to find out the best one practically impossible when there are lots of filters available. In this paper, a genetic algorithm is used to search filters of the proper type and order.

Fig. 3 shows the procedure of the proposed method which also presents the process of evaluating fitness. In each generation, the fitness of chromosome is evaluated by using the fitness function, and chromosomes with higher fitness are stochastically selected and applied with genetic operators such as crossover and mutation to reproduce the population of the next generation. Elitist-strategy [20] that always keeps the best chromosome found so far is used. Chromosomes are represented as simple numbers corresponding with individual filters, and Table 1 shows the type and effect of 71 individual filters.

Chromosomes with the length of five represent a set of filters. Fig. 4 shows the structure of chromosomes and the examples of genetic operators such as crossover and mutation.

The fitness of an individual is estimated by the performance of singularity extraction using the Poincare index. The Poincare index extracts singularity using the orientation field which is calculated for each block. Singularity is classified into the core and delta, and these two points do not lie together in the same location. Let  $S_d = \{s_{d1}, s_{d2}, \dots, s_{dn}\}$  be the set of  $n$  singularity points detected by the singularity extraction algorithm, and  $S_e = \{s_{e1}, s_{e2}, \dots, s_{em}\}$  be the set of  $m$  singularity points identified by human experts in an input fingerprint image. The following sets are defined.

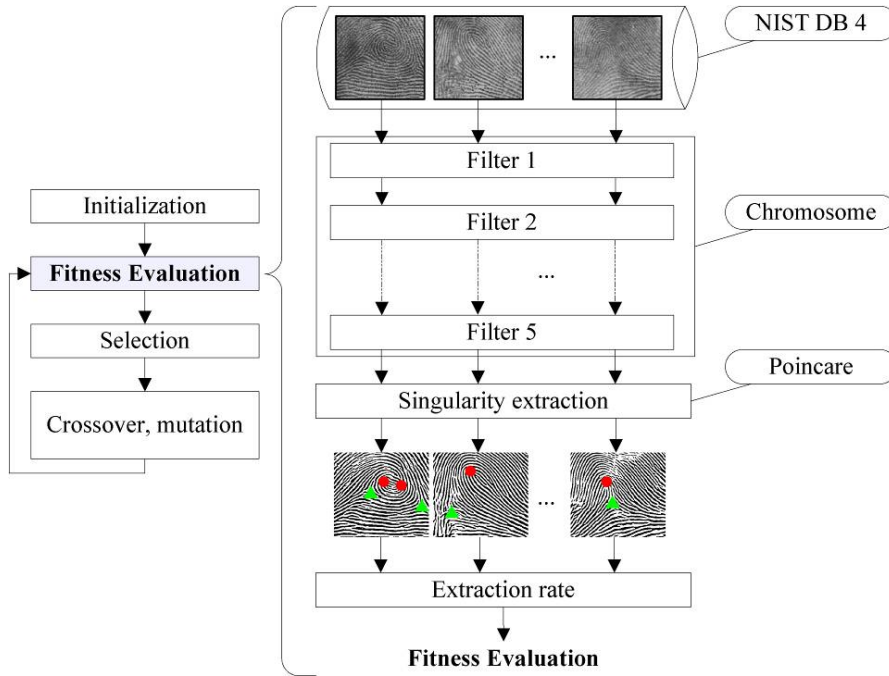


Fig. 3. The process of evaluating fitness (fitness function)

Table 1. The effect of various image filter

| Group       | Filter     | Type     | Effect   | Number |
|-------------|------------|----------|--|--------|
| Histogram   | Brightness | 3 values | Brightness value control                             | 1~3    |
|             | Contrast   | 3 values | Contrast value control                               | 4~6    |
|             | Stretch    | -        | Stretching histogram of images                       | 7      |
|             | Equalize   | -        | Equalization histogram of images                     | 8      |
|             | Logarithm  | -        | Logarithm histogram of images                        | 9      |
| Mask        | Blur       | 6 masks  | Smoothing images                                     | 10~15  |
|             | Sharper    | 4 masks  | Sharpen images                                       | 16~19  |
|             | Median     | 10 masks | Noise elimination                                    | 20~29  |
| Morphology  | Erosion    | 10 masks | Elimination of single-pixel bright spots from images | 30~39  |
|             | Dilation   | 10 masks | Elimination of single-pixel dark spots from images   | 40~49  |
|             | Opening    | 10 masks | Clean up images with noise                           | 50~59  |
|             | Closing    | 10 masks | Clean up images with object holes                    | 60~69  |
| Fingerprint | Gabor      | -        | Ridge amplification with orientation field           | 70     |
| None        |            |          |  | 0      |

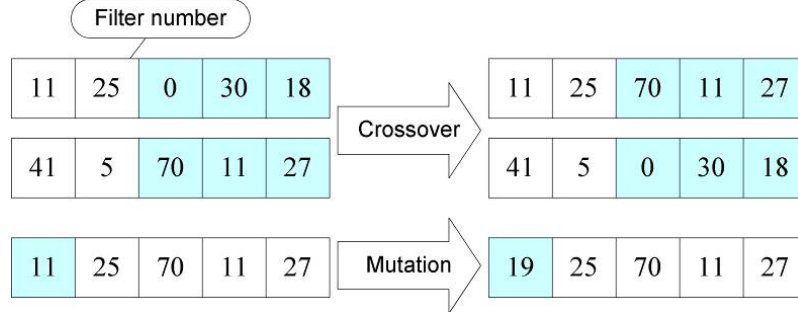


Fig. 4. The structure of chromosome and genetic operators

- Paired singularity ( $p$ ): A set of the singularity points that  $s_d$  and  $s_e$  are paired if  $s_d$  is located within the tolerance (20 pixels) centered around  $s_e$ .
- Missing singularity ( $a$ ): A set of the points that are located within the tolerance distance from singularity  $s_e$  but not singularity  $s_d$ , which means that the singularity extraction algorithm cannot detect the point.
- Spurious singularity ( $b$ ): A set of the points that are located within the tolerance distance from singularity  $s_d$  but not singularity  $s_e$ , which is detected by the singularity extraction algorithm, but not real singularity.

The missing rate of singularity is estimated by the equation (1), the spurious rate is estimated by the equation (2), and the accuracy rate is estimated by the equation (3) with N samples.

$$P(a) = \frac{\sum_{i=1}^N n(a_i)}{\sum_{i=1}^N n(S_{ei})} \quad (1)$$

$$P(b) = \frac{\sum_{i=1}^N n(b_i)}{\sum_{i=1}^N n(S_{di})} \quad (2)$$

$$P(p) = 1 - \frac{\sum_{i=1}^N (n(a_i) + n(b_i))}{\sum_{i=1}^N (n(S_{di}) + n(S_{ei}))} \quad (3)$$

The accuracy of singularity is used as the fitness function of the genetic algorithm, where an individual that shows better enhancement performance obtains a higher score.

## 4 Experiments

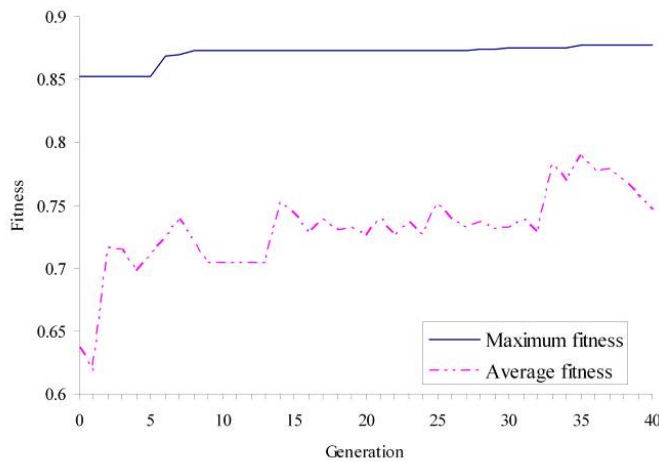
The NIST Special Database 4 was used [21] to verify the proposed method. The NIST DB 4 consists of 4000 fingerprint images (2000 pairs). In the experiments, the training set was composed of the first 2000 images, f0001~f2000, and the test set consisted of the other 2000 images, s0001~s2000. In the database, 7308 singularities are manually marked by human experts, including 3665 on the training set and 3642 on the test set.

### 4.1 Analysis of the Process of Evolution

Table 2 shows the initial values of parameters in the experiment. The 40th generation results in a rise of 0.02 for the maximum fitness and a rise of 0.3 for the average fitness of the population which is 30 individuals. Fig. 5 shows the change of maximum and average fitnesses in each generation, where the maximum fitness increases steadily and the average fitness also shows a rise.

**Table 2.** The initial values of parameters

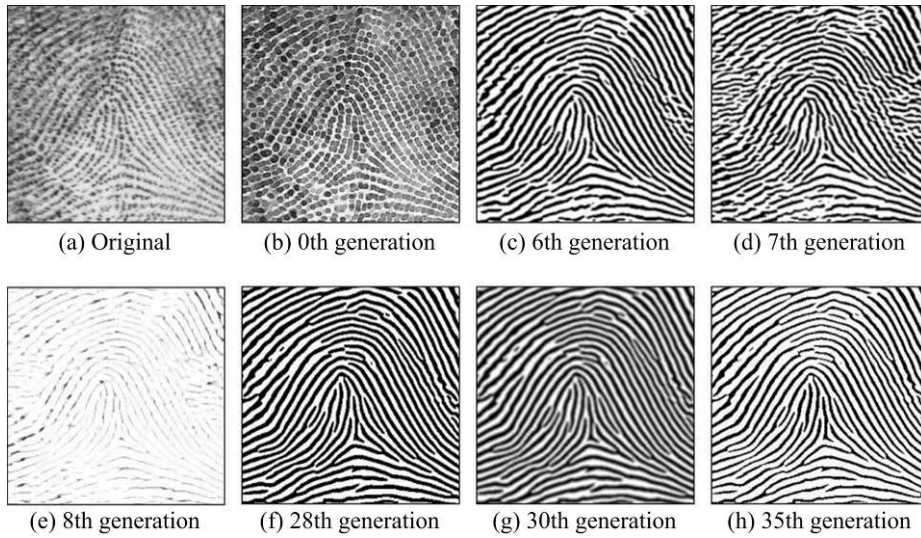
| Parameter         | Value |
|-------------------|-------|
| Generation        | 40    |
| Population        | 30    |
| Chromosome length | 5     |
| Selection rate    | 0.7   |
| Crossover rate    | 0.7   |
| Mutation rate     | 0.05  |
| Elitist-strategy  | Yes   |



**Fig. 5.** The maximum and average fitnesses in each generation

**Table 3.** The number and type of image filters used in constructing a set of filters

| generation | Filter #, type |                    |                   |                  |                  |                 |      |                   |                   |                    |
|------------|----------------|--------------------|-------------------|------------------|------------------|-----------------|------|-------------------|-------------------|--------------------|
|            | 0              | 11                 | Lowpass<br>3×3 #2 | 25               | Median<br>3×3 #3 | 0               | NULL | 30                | Erosion<br>3×3 #1 | 18                 |
| 6          | 11             | Lowpass<br>3×3 #2  | 25                | Median<br>3×3 #3 | 70               | Gabor<br>filter | 11   | Lowpass<br>3×3 #2 | 27                | Median<br>1×3      |
| 7          | 19             | Highpass<br>3×3 #4 | 25                | Median<br>3×3 #3 | 70               | Gabor<br>filter | 11   | Lowpass<br>3×3 #2 | 27                | Median<br>1×3      |
| 8          | 19             | Highpass<br>3×3 #4 | 25                | Median<br>3×3 #3 | 70               | Gabor<br>filter | 11   | Lowpass<br>3×3 #2 | 46                | Dilation<br>5×5 #4 |
| 28         | 14             | Gaussian<br>3×3    | 25                | Median<br>3×3 #3 | 70               | Gabor<br>filter | 70   | Gabor<br>filter   | 68                | Closing<br>1×3     |
| 30         | 14             | Gaussian<br>3×3    | 25                | Median<br>3×3 #3 | 70               | Gabor<br>filter | 70   | Gabor<br>filter   | 12                | Lowpass<br>5×5     |
| 35         | 14             | Gaussian<br>3×3    | 25                | Median<br>3×3 #3 | 70               | Gabor<br>filter | 70   | Gabor<br>filter   | 48                | Dilation<br>3×3    |



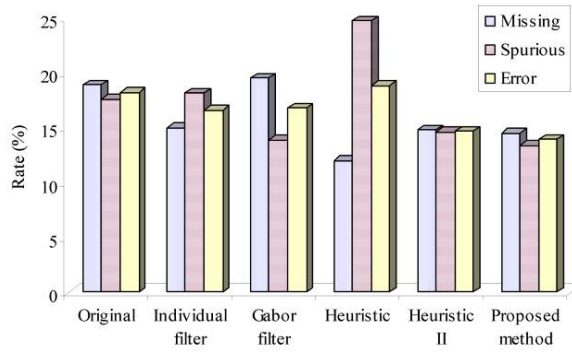
**Fig. 6.** Results of evolutionary filters

Table 3 shows filters obtained through the evolution. The Gabor filter is included in all the filters except for that of randomly initialized. These obtained filters are divided into the front part and rear part by the Gabor filter. The Gabor filter has the effect of ridge amplification with the orientation field, and orientation field correctly extracted can maximize the performance singularity extraction. Filters of the front part usually concern in the orientation field, and filters of the rear part effect an improvement for the result image of the Gabor filter. Finally, filter is obtained, which

composes of Gaussian filter, median filter, two Gabor filters, and dilation. The input image is smoothed by the Gaussian filter, and impulse noise spikes of the image are removed by the median filter. The Gabor filter effects to correctly calculate the orientation field with ridge amplification. The dilation operation is used to remove small anomalies, such as single-pixel holes in objects and single-pixel-wide gaps of the image. It also has effect of thinning the ridges of images through the wider valleys of image. Fig. 6 shows example images obtained after applying filters.

**4.2 Singularity Extraction**

In the experiments, the error rate of singularity extraction over all individual filters was investigated, and we obtained 5 good filters that were ‘median 3×3 rectangle mask filter,’ ‘closing 3×3 X mask operator,’ ‘Gaussian 3×3 mask filter,’ ‘Gabor filter,’ and ‘closing 3×3 diamond mask operator.’ The heuristic filter is composed of these 5 filters, and the heuristic filter II has the reverse order of the previous one. Fig. 7 shows the comparison of various filters. The error rate of original was 18.2%, whereas individual



**Fig. 7.** The performance comparison with other filters

**Table 4.** Type and error rate of other filters

| Filter          | Filter type          |               |              |               |                      | Error rate |
|-----------------|----------------------|---------------|--------------|---------------|----------------------|------------|
| Original        | NULL                 |               |              |               |                      | 18.2%      |
| Individual      | Closing Diamond 3×3  |               |              |               |                      | 16.6%      |
| Gabor           | Gabor Filter         |               |              |               |                      | 16.7%      |
| Heuristic       | Median Rectangle 3×3 | Closing X 3×3 | Gaussian 3×3 | Gabor Filter  | Closing Diamond 3×3  | 18.8%      |
| Heuristic II    | Closing Diamond 3×3  | Gabor Filter  | Gaussian 3×3 | Closing X 3×3 | Median Rectangle 3×3 | 14.7%      |
| Proposed method | Gaussian 3×3         | Median X 3×3  | Gabor Filter | Gabor Filter  | Dilation 1×3         | 13.9%      |

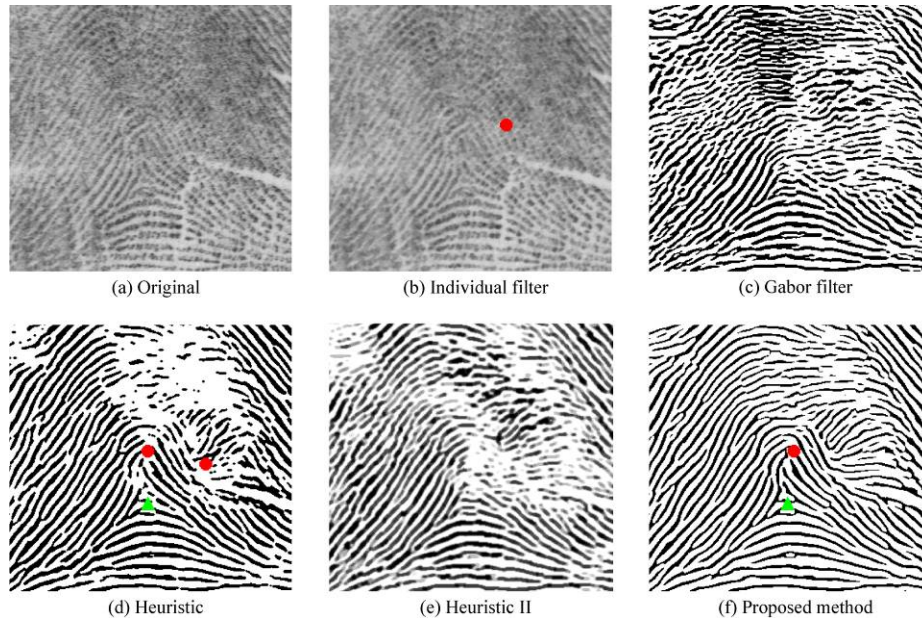


Fig. 8. Examples of various filters (● = core, ▲ = delta)

filters and the Gabor filter produced 16.6% and 16.7% error rates, respectively. The heuristic II filter yielded 14.7% error rate, while the proposed method obtained an error rate of 13.9%. The proposed method shows better performance in singularity extraction than the filters designed heuristically (Table 4).

The fingerprint image in Fig. 8 has one core and one delta. Fig. 8(a) shows the original image and singularity is not detected by the extraction algorithm. Individual filter that is a closing operation eliminates single-pixel dark spots from the image and smoothes it, but the extraction algorithm detects a spurious singularity because of unclear orientation on upper right-hand side field (Fig. 8(b)). The image is not enhanced well with the Gabor filter because the orientation field is not good (Fig. 8(c)). The extraction algorithm detects not all singularity but spurious singularity with the heuristic filter because of many blank spaces (Fig. 8(d)). The extraction algorithm with the proposed method detects no missing and spurious singularity (Fig. 8(f)).

## 5 Conclusions

It is important to detect singularities, which are special features of fingerprint, but limited in quality of fingerprint images. Image enhancement is required for correct extraction. In this paper, a genetic algorithm is used to obtain a combination of various individual filters for better performance in singularity extraction. In the experiments of NIST DB 4, the filter obtained shows better performance than the other filters.

In future work, we would like to apply the proposed method to the other fingerprint image databases. By changing the fitness function of the genetic algorithm, the method for better performance of identification and classification of fingerprints will be also investigated. Since the proposed method does not need any expert knowledge, we can also apply the method to various fields of image processing.

## Acknowledgements

This work was supported by the Korea Science and Engineering Foundation (KOSEF) through the Biometrics Engineering Research Center (BERC) at Yonsei University.

## References

- [1] N. Ratha, and R. Bolle, *Automatic Fingerprint Recognition Systems*, Springer-Verlag, New York, 2004.
- [2] A. K. Jain, L. Hong, and R. Bolle, "On-line fingerprint verification," *IEEE Transactions on Pattern Analysis and Machine Intelligence*, vol. 19, no. 4, pp. 302-314, 1997.
- [3] A. M. Bazen, and S. H. Gerez, "Systematic methods for the computation of the directional fields and singular points of fingerprints," *IEEE Transactions on Pattern Analysis and Machine Intelligence*, vol. 24, no. 7, pp. 905-919, 2002.
- [4] A. M. Bazen, and S. H. Gerez, "Segmentation of fingerprint images," *In Proc. ProRISC2001 Workshop on Circuits, Systems and Signal Processing*, Veldhoven, The Netherlands, pp. 276-280, 2001.
- [5] L. Hong, Y. Wan, and A. Jain, "Fingerprint image enhancement: Algorithm and performance evaluation," *IEEE Transactions on Pattern Analysis and Machine Intelligence*, vol. 20, no. 8, pp. 777-789, 1998.
- [6] J. Yang, L. Liu, T. Jiang, and Y. Fan, "A modified Gabor filter design method for fingerprint image enhancement," *Pattern Recognition Letters*, vol. 24, pp. 1805-1817, 2003.
- [7] S. Greenberg, M. Aldadjem, and D. Kogan, "Fingerprint image enhancement using filtering techniques," *Real-Time Imaging*, vol. 8, pp. 227-236, 2002.
- [8] E. Zhu, J. Yin, and G. Zhang, "Fingerprint enhancement using circular Gabor filter," *International Conference on Image Analysis and Recognition*, pp. 750-758, 2004.
- [9] D. Goldberg, *Genetic Algorithm in Search, Optimization and Machine Learning*, Addison Wesley, 1989.
- [10] L. M. Schmitt, "Theory of genetic algorithms," *Theoretical Computer Science*, vol. 259, pp. 1-61, 2001.
- [11] S. B. Cho, "Emotional image and musical information retrieval with interactive genetic algorithm," *Proceedings of the IEEE*, vol. 92, no.4, pp. 702-711, 2004.
- [12] N. R. Harvey, and S. Marshall, "The use of genetic algorithms in morphological filter design," *Signal Processing: Image Communication*, vol. 8, pp. 55-71, 1996.
- [13] N. Yager, and A. Admin, "Fingerprint classification: A review," *Pattern Analysis and Application*, vol. 7, pp. 77-93, 2004.
- [14] M. M. S. Chong, T. H. Ngee, L. Jun, and R. K. L. Gay, "Geometric framework for fingerprint image classification," *Pattern Recognition*, vol. 30, pp. 1475-1488, 1997.
- [15] Q. Zhang, and H. Yan, "Fingerprint classification based on extraction and analysis of singularities and pseudo ridges," *Pattern Recognition*, vol. 37, pp. 2233-2243, 2004.

- [16] A. K. Jain, S. Prabhakar, and L. Hong, "A multichannel approach to fingerprint classification," *IEEE Transactions on Pattern Analysis and Machine Intelligence*, vol. 21, no. 4, pp. 348-359, 1999.
- [17] R. Cappelli, A. Lumini, D. Maio, and D. Maltoni, "Fingerprint classification by directional image partitioning," *IEEE Transactions on Pattern Analysis and Machine Intelligence*, vol. 21, no. 5, pp. 402-421, 1999.
- [18] A. Ross, A. Jain, and J. Reisman, "A hybrid fingerprint matcher," *Pattern Recognition*, vol 36, pp.1661-1673, 2003.
- [19] R. Gonzalez, and R. Woods, *Digital Image Processing*, Addison Wesley, Reading, MA, 1992.
- [20] L. M. Schmitt, "Theory of genetic algorithms II: Models for genetic operators over the string-tensor representation to populations and convergence to global optima for arbitrary fitness function under scaling," *Theoretical Computer Science*, vol. 310, pp. 181-231, 2004.
- [21] C. Watson, and C. Wilson, *NIST Special Database 4. Fingerprint Database*. National Institute of Standard and Technology, 1992.